THICKNESS SCALING FOR ARC DISCHARGES ON ELECTRON-BEAM-CHARGED DIELECTRICS*

K.G. Balmain, A. Battagin, and G.R. Dubois
Department of Electrical Engineering
University of Toronto
Toronto, Canada M5S 1A4

Abstract

A study of arc discharges on various thicknesses of electron-beam-charged Mylar, FEP Teflon and Kapton shows that the peak substrate current and the energy dissipated in a load resistor both exhibit maxima at a particular thickness of the order of 50 μm, for one set of experiment parameters. The experiments also show that, as thickness increases, this particular thickness is the transition from near-constant to decreasing released charge, and, for Mylar, from decreasing to near-constant arc duration. This transition is interpreted as being caused primarily for thin specimens by punchthrough formation and possibly influenced by the transition from conduction-dominated to emission-dominated charging. Additional low-energy ion exposure is shown to weaken and sometimes eliminate the arc discharges without radically altering the thickness scaling. At low fluxes, the incident ions are focussed into a central spot.

Introduction

The accumulation of charge and the threat of arc breakdown on exposed spacecraft dielectric materials have been a matter of concern to spacecraft designers for about fourteen years, and the first journal review on the subject was published by Rosen in 1976 [1]. In subsequent years, extensive laboratory simulation has been carried out in order to study both the charge accumulation and arc breakdown processes, processes which have been reviewed recently by Frederickson [2]. Most of the laboratory experimentation has been done on sheets of polymeric materials which are used for spacecraft thermal control, such as Kapton and Mylar thermal blankets and Teflon second-surface mirrors. The thicknesses used ranged from 12.5 to 125 μm, but to date there has been no attempt to establish the inter-relationships between phenomena observed on specimens of different thicknesses.

This paper addresses part of this problem, namely the variation with specimen thickness of the electrical properties of arc discharges, under exposure to a monoenergetic electron beam of fixed current density, combined with a low energy ion beam. If one wished to model accurately the magnetospheric environment, one would have to use appropriate broad-spectrum, low-current-density sources of both electrons and ions, and the results of such an experiment would no doubt be different from those to be presented here. The present objective is more limited, being to contribute to the process of tying together the many monoenergetic-electron experiments that have been done, in the belief that understanding those experiments is a necessary prerequisite to the study of more complicated situations.

The experiments to be described involve a polymer sheet lying on a flat metal substrate and covered by a close-fitting metal mask with a circular aperture. The electrical quantities measured directly are the substrate and mask currents as functions of time, the method employed being to measure the voltages across two low-value resistors connected respectively to the substrate and the mask.

*Work supported by the U.S. Air Force Weapons Laboratory through AFOSR Grant 84-0342, and by the Natural Sciences and Engineering Research Council of Canada, through Operating Grant A-4140.

Theoretical Considerations

A dielectric sheet over a ground plane and in a vacuum accumulates surface charge when exposed to an incident electron beam. As time progresses, if not interrupted by electrical breakdown, the surface charge and potential both approach an equilibrium state which corresponds to current balance involving the incident electrons, the backscattered electrons, the secondary emission from the dielectric, and the conduction through the dielectric. It has been shown [3] that, for a monoenergetic incident beam in which the current density J_i actually reaches the dielectric, the equilibrium state may be dominated either by conduction or by emission, the transition between these two states being given for Teflon and for a 20 kV beam accelerating voltage by

$$\frac{J_i\, d}{g} \simeq 2 \times 10^4 \text{ volts} \tag{1}$$

in which d is the dielectric thickness and g is its conductivity. The transition is not sharp but occurs gradually over as much as an order of magnitude in $J_i d/g$, and the transition point is not significantly different for other good dielectrics such as Kapton. For a constant beam accelerating voltage, the conduction-limited state is characterized by the surface potential V being proportional to $J_i d/g$ through the relation

$$V = (1\text{-SE-BS})\ J_i d/g \tag{2}$$

in which SE and BS are the secondary emission and backscatter coefficients. The emission-limited state is characterized by the surface potential V being constant, that is

$$eV = (\text{BE}-\text{KE}_2) \tag{3}$$

where BE is the beam energy and KE_2 is the second-unity-crossover emission energy at which SE+BS = 1.

Regarding the assumed uniformly charged dielectric as a parallel-plate capacitor, one may take the charge to be Q=CV where the capacitance $C = \varepsilon A/d$, A being the area, and one may take the stored energy to be $E_o=CV^2/2$. These may be written as follows, displaying their dependence on V and d:

$$Q = \varepsilon A\ V/d \tag{4}$$

$$E_o = \tfrac{1}{2}\varepsilon A\ V^2/d \tag{5}$$

It may be assumed that a discharge involves total charge cleanoff, which is known to be approximately true for the strongest discharges; then Q is the total charge flow to ground via the replacement current I from the metal substrate supporting the dielectric. The stored energy E_o is generally much greater than the energy E dissipated in a low-value load resistor connecting the substrate to ground. Making the tentative assumption $E \propto E_o$, we would have

$$E \propto V^2/d \tag{6}$$

The released charge is given by $Q = \int I\, dt$. If we assume I(t) is a symmetric triangle function with peak current I_p and duration between half-current points given by T, then

$$Q = I_p T \quad (7)$$

With the same triangular current pulse passing through a load resistor of R ohms, it is straightforward to show that

$$E = (2R/3)\, I_p^2\, T \quad (8)$$

The following relations are deduced from (7) and (8):

$$E/Q = (2R/3)\, I_p \quad (9)$$

$$Q^2/E = (3/2R)\, T \quad (10)$$

Equations (4), (6), (9) and (10) plus the fact that, for constant incident current density J_i, conduction-limiting implies $V \propto d$ and emission-limiting implies $V = $ constant, together make it possible to estimate the thickness dependence of the properties of the arc discharge as shown in the following Table. In the table, the behavior of the released charge Q is independent of any assumptions related to E, I_p or T. However the predicted behavior of E, I_p and T with variations in thickness d depends on the assumption $E \propto E_o$. Also shown in the table are the emission-limited results for the alternative assumptions $I_p \propto 1/d$ and $I_p \propto 1/d^2$ which are based on measurements to be presented.

Table I

Conduction-dominated charging (thin dielectric)	Emission-dominated charging (thick dielectric)		
$E \propto E_o$	$E \propto E_o$	$I_p \propto 1/d$	$I_p \propto 1/d^2$
Q = constant	$Q \propto 1/d$	$Q \propto 1/d$	$Q \propto 1/d$
$E \propto d$	$E \propto 1/d$	$E \propto 1/d^2$	$E \propto 1/d^3$
$I_p \propto d$	I_p = const.	$I_p \propto 1/d$	$I_p \propto 1/d^2$
$T \propto 1/d$	$T \propto 1/d$	T = const.	$T \propto d$

This table shows that, as thickness increases, the released charge Q will change from a constant to a decreasing quantity independent of any assumptions on E or I_p. This table also suggests that the energy E dissipated in a load resistor will be a maximum at a transition thickness given by

$$d \simeq 2 \times 10^4\ g/J_i \quad (11)$$

The peak current I_p and the pulse duration T may also exhibit thickness dependence.

Experiment Parameters

A beam accelerating voltage of 20 kV was selected because of the existence of data on many experiments at this voltage. A beam current density J_b of 25 nA/cm² was chosen to allow the accumulation of an adequate quantity of discharge data in a reasonable time, although this current density is one to two orders of magnitude too high to simulate conditions around spacecraft in synchronous orbit. In the laboratory, the actual incident current density is lower than the beam current density due to beam spreading, a reasonable approximation for this case being $J_i = 0.4\ J_b$ [4]. The low-field conductivity of FEP Teflon at room temperature and low field strength could be of the order of 10^{-20} (ohm-cm)$^{-1}$ rising to a value perhaps as high as 10^{-15} (ohm-cm)$^{-1}$ at elevated temperature (~ 400 K) and as the internal electric field approaches breakdown strength [4,5]. Under the extreme highest-conductivity conditions the transition thickness would be

$$d \simeq 2 \times 10^4\ g/J_i$$

$$\simeq 20\ \mu m$$

(with similar results expected for Mylar [5]) which is just within the range of available material thicknesses, these being 12.5, 25, 50, 75 and 125 µm. The conductivity for Kapton could be of the same order of magnitude or higher [6], but at room temperature. Trying to predict the transition thickness is obviously very difficult due to extreme uncertainty about the conductivity at the point of breakdown and also due to some uncertainty about the degree of beam spreading.

The experimental configuration was the same as used in the past [7]: it consisted of the dielectric sheet specimen sandwiched between a flat metal substrate and a metal aperture mask with a bevelled-edge circular aperture of area 15.9 cm². The substrate and mask were connected to the metal vacuum chamber walls ("ground") through individual 2.5 ohm resistors, the resistor voltages being used to deduce the substrate and mask currents during a discharge. The electron beam was magnetically deflected through approximately 90 degrees to permit direct viewing and photography of the specimen. Ion exposure was also available using a small Lithium oven and 100-volt-accelerator ion extractor which produced a broad flood beam of ions at a current density equal to 10% of the electron current density, comparable to relative ion current densities used in past work [8] and existing in the magnetosphere [9,10,11]. Before the experiments, multiple Faraday cups were used to measure the incident current density distribution which was established as uniform over the mask aperture to within ± 15%. During each experiment, a single Faraday cup mounted just to the side of the mask aperture was used to monitor the incident current density which was maintained constant to within ± 10%. The dielectric specimens were used in the state "as received from the manufacturer" but it was also confirmed by a few experiments that there was no noticeable effect due to cleaning the specimens with trichloroethylene in a vapor degreaser. The vacuum pressure was always lower than 9×10^{-6} torr.

The primary measurement during an arc discharge was current I as a function of time, the peak value being designated I_p. The current was integrated to give the released charge Q, and the square of the current multiplied by the resistance (R = 2.5 ohms) was integrated to give the energy E. The current pulse duration T was measured as the time between the $I = \frac{1}{2} I_p$ points.

Experiment Results

The results for thickness scaling are presented in Figs. 1 to 4. Each graph displays up to four data curves and includes short-form designations for the curves, the short-forms having the following meanings:

Sub:e	means	Substrate: electrons only.
Mask:e	"	Mask: electrons only.
Sub:e+i	"	Substrate: electrons plus ions.
Mask:e+i	"	Mask: electrons plus ions.

The word "maximum" over the Q, E, and I_p graphs is an indicator that only the strongest discharge pulse observed for each case contributes to the data presented. Graphs for data averaged over all discharges were also plotted but are not shown. They were generally similar in shape but were significantly reduced in magnitude by the occurrence of punchthroughs after a few discharges. Among the "maximum" discharges analyzed the only cases that exhibited punchthroughs were the following:

12.5 μm Teflon with electrons only (8 punchthroughs),

25 μm Teflon with electrons only (4 punchthroughs),

12.5 μm Teflon with electrons and ions (2 punchthroughs),

and 12.5 μm Mylar with electrons only (1 punchthrough)

The pulse duration graphs displayed are of averaged data because the pulse duration is determined by arc propagation velocity and therefore is not strongly influenced by the occurrence of punchthroughs. Pulse duration graphs were plotted (but are not shown) for those discharges having the largest peak currents: these graphs were found to be generally similar to the average pulse duration graphs.

The Mylar and FEP Teflon specimen thicknesses were 12.5, 25, 50, 75 and 125 μm, and the Kapton specimen thicknesses included all of these except 12.5 μm. On the graphs, the absence of data for an available thickness indicates that no discharges were observed after an exposure period of at least 30 minutes. For example, no discharges were observed on any of the Kapton specimens under exposure to electrons plus ions, nor on the 25 μm Kapton with electron-only exposure. Also, the 12.5 μm Mylar did not discharge under exposure to electrons plus ions.

Figures 5 and 6 show typical arc discharges on the same specimen of 25 μm Mylar, under electron-only irradiation. A punchthrough is clearly identifiable as a bright spot, and essentially the whole area is covered by the arc. Figure 7 shows a luminescence pattern with 10% ion flux, and Fig. 8 shows an arc occurring under an ion flux of about 3%.

Discussion of Results: Electrons Only

The charge graphs appear to agree well with the rudimentary theory presented, and there is also a measure of apparent qualitative agreement for thin specimens under the assumption that the energy E dissipated in a substrate load resistor is proportional to the stored energy E_o. For thick specimens the slopes of the log-log graphs of measured data are shown in Table II, with the two values in parentheses being those for the initial assumptions $I_p \propto 1/d$ and $I_p \propto 1/d^2$.

Table II

Measured (predicted) substrate graph slope magnitudes for the thickest specimens irradiated with electrons only

	Charge	Energy	Peak Current
Mylar	1.1 (1,1)	3.2 (2,3)	2.0 (1,2)
Teflon	1.1 (1,1)	2.7 (2,3)	1.4 (1,2)
Kapton	1.2 (1,1)	2.8 (2,3)	1.3 (1,2)

For thin specimens the comparison is more random and is not shown. For the substrate discharge pulse duration graphs (electrons only), there is not a consistent similarity between the experiments and the predictions.

The predictions summarized in Table I are based on the premise that the specimen charges up almost to the equilibrium state before a discharge occurs. If the first discharge on a previously untested specimen exhibits a punchthrough, then experience shows that the discharge is weaker than might be expected, presumably because the discharge was triggered early by an initial breakdown at a point of weakness (such as a gaseous inclusion) which results in specimen perforation at that point. Thus one associates punchthrough occurrence with premature and therefore relatively weak arc discharges. The punchthrough occurrences already noted could have contributed to the weaker discharges for the thinnest specimens of both Mylar and Teflon, and therefore it is not at all certain that the measured transitions in the 25 to 50 μm range were actually caused by the theoretical transition between conduction and emission domination in the charging process, a transition which could be pushed as high as 20 μm thickness only by the assumption of improbably high conductivity caused by temperatures of the order of 400K. Rather, the experimental evidence of punchthrough formation suggests that localized material weakness which affects thin specimens preferentially is the most likely cause of the observed variation of discharge properties for the thinner specimens. For the thicker specimens, emission-dominated charging appears to be the main factor controlling the variation with thickness of the discharge properties, because the released charge was found to vary with thickness as predicted, independent of whether the initial assumption was $E \propto E_o$ or an observed I_p dependence. The measured variation with thickness of energy dissipated in the load resistor appears to require the initial assumption that the peak current is proportional to something between $1/d$ and $1/d^2$. The initial assumption $E \propto E_o$ appears to be generally inappropriate for thick specimens, although it does predict correctly the slope of the pulse duration graph for Teflon.

The measured variation of pulse duration with thickness indicates that the thickness of the specimen influences arc velocity. Under electron-only exposure the velocities (mask radius divided by duration) range from 0.5×10^5 to 5.6×10^5 m/s for Mylar, from 1.8×10^5 to 7.5×10^5 m/s for Teflon, and from 2.8×10^5 to 5.0×10^5 m/s for Kapton. Arc velocity increase with increasing deposited charge in very thick specimens has been reported by Erickson and Oakley [12] and by Cooke et al. [13] for very high-energy, short-duration electron exposure but the great differences in experimental circumstances make comparison with the present work difficult.

Discussion of Results: Electrons Plus Ions

The electron-only arc photographs of Figs. 5 and 6 (both on the same Mylar specimen) show arcs that cover the entire exposed dielectric in spite of the existence of localized triggering at a punchthrough. Figure 7 is a photograph of luminescence only, in the absence of any arc, but for combined electron plus 10% ion exposure. On the photograph there are two bright regions which require explanation. The upper bright region is the specular reflection of the very dim red light from the small Lithium oven ion gun. The lower bright region disappears slowly after the ion gun is turned off and expands when the ion current density is increased. This bright region is therefore interpreted as a region of steady-state ion neutralization of embedded electron charge, which permits the electrons to approach the dielectric unimpeded and produce the bright region by impact luminescence. The bright region is approximately centrally located because the embedded electrons produce high transverse edge fields which draw the low energy ions radially inward from the specimen edge before drawing them to the surface in the middle region of the specimen. If this interpretation were correct, then, in order for steady-state neutralization to occur in the bright region when the incident ion flux density is 10% of the electron flux density, the exposed specimen area would have to be 10 times the bright-region area. In fact the area ratio is about 13, close enough to 10 to lend support to the explanation offered above.

Figure 8 shows an arc on a specimen exposed to a somewhat lower incident ion current density which was not accurately measured but estimated at 3% of the electron current density. In the photograph there is an evident tendency for the arc to avoid a central region whose area is somewhat smaller than the bright region already discussed, a phenomenon consistent with the lower ion current density creating a smaller charge-neutral region which cannot support a propagating arc discharge.

Conclusions

Under electron-only exposure at one value of incident current density (25 nA/cm²), the properties of beam-induced arc discharges on polymer sheets scale with sheet thickness in a manner which is regular and similar from one material to another indicating that a transition occurs around 50 μm thickness. For thick sheets, the released charge scales in accordance with a prediction assuming that the charge accumulation process is emission-dominated and that the released charge is proportional to the accumulated charge. A corresponding, simple prediction of scaling laws for peak current and energy dissipated in a load resistor was not achieved due to insufficient knowledge of the discharge mechanism, although a measure of consistency between peak current and energy scaling was established for thick specimens.

For thin specimens exposed to electrons only, the released-charge scaling levels off approximately as predicted by assuming that the charge accumulation process is dominated by the conductivity of the polymer, including nonlinear conductivity, but such conductivity would have to be improbably high to produce a transition between conduction and emission domination in the 20-50 μm range. A much more likely explanation based on observation is that the levelling out of released charge for thin specimens was caused by punchthrough formation and subsequent premature discharging. As for thin-specimen peak current and energy scaling, a measure of qualitative agreement with experiment was achieved by assuming that the energy dissipated is proportional to the stored energy but, again, lack of understanding of the discharge mechanism prevents the establishment of a well-founded, simple prediction.

Under electron-plus-ion exposure, a relatively bright, steady, luminescent spot was observed in the central region of the specimen. This spot was avoided by discharge arcs and therefore was interpreted as an area of ion impact and electron-ion charge neutralization. The reduction in arc strength due to the ion exposure was too great to be explained simply by postulating that the effective specimen area was reduced by the size of the ion spot. Rather, it is likely that enough ions fall outside the spot area to reduce significantly the net charge accumulated there. With ions, the arc discharges are weakened and sometimes eliminated, but the thickness-scaling graphs are not greatly changed in shape. Insofar as spacecraft are concerned, it appears that low energy ions from the ambient plasma could be drawn in to neutralize partially any exposed electron-charged dielectrics.

References

[1] A. Rosen, "Spacecraft charging by magnetospheric plasmas," IEEE Trans. Nucl. Sci., vol.NS-23, no.6, pp. 1762-1768, Dec. 1976.

[2] A.R. Frederickson, "Electric discharge pulses in irradiated solid dielectrics in space," IEEE Trans. Elect. Insulation, vol.EI-18, no.3, pp. 337-349, June 1983.

[3] R.D. Reeves and K.G. Balmain, "Two-dimensional electron beam charging model for polymer films, IEEE Trans. Nucl. Sci., vol.NS-28, no.6, pp. 4547-4552, Dec. 1981.

[4] R.D. Reeves, Two-Dimensional Electron Beam Charging Model for Polymer Films, M.A.Sc. Thesis, Dept. of Elect. Engrg., Univ. of Toronto, 1981.

[5] V. Adamec and J.H. Calderwood, "Electrical conduction in dielectrics at high fields," Journal of Physics D, vol.8, pp. 551-560, 1975.

[6] J.B. Reagan, R.E. Meyerott, E.E. Gaines, R.W. Nightingale, P.C. Filbert, and W.L. Imhof, "Space charging currents and their effects on spacecraft systems," IEEE Trans. Elect. Insul., vol.EI-18, no.3, pp. 354-365, June 1983.

[7] K.G. Balmain and W. Hirt, "Dielectric surface discharges: dependence on incident electron flux," IEEE Trans. Nucl. Sci., vol.NS-27, no.6, pp. 1770-1775, Dec. 1980.

[8] M. Gossland and K.G. Balmain, "Incident ion effects on polymer surface discharges," IEEE Trans. Nucl. Sci., vol.NS-30, no.6, pp. 4302-4306, Dec. 1983.

[9] S.E. DeForest, "Spacecraft charging at synchronous orbit," J. Geophys. Res., vol.77, pp. 651-659, Feb. 1972. See also E.C. Whipple, "Potentials of surfaces in space," Rep. Prog. Phys., vol.44, pp. 1197-1250, 1981.

[10] J.B. Reagan, R.W. Nightingale, E.E. Gaines, R.E. Meyerott, and W.L. Imhof, "Role of energetic particles in charging/discharging of spacecraft dielectrics," Spacecraft Charging Technology 1980, NASA CP 2182/AFGL-TR-81-0270, pp. 74-85.

[11] J. Wilkenfeld, C. Mallon, and J. Horne, "Conduction and charge storage in electron-irradiated spacecraft insulators," RADC-TR-81-198, July 1981.

[12] L.M. Erickson and D.C. Oakley, "Time-resolved voltage breakdown in various insulators due to 2-MeV electrons," Lawrence Livermore Laboratory Report UCRL-51372, 5 April 1973.

[13] C.M. Cooke, E. Williams, and K.A. Wright, "Electrical discharge propagation in space-charged PMMA," Conference Record of the 1982 IEEE International Symposium on Electrical Insulation, pp. 95-101.

Fig.1(a) *MYLAR MAXIMUM CHARGE*

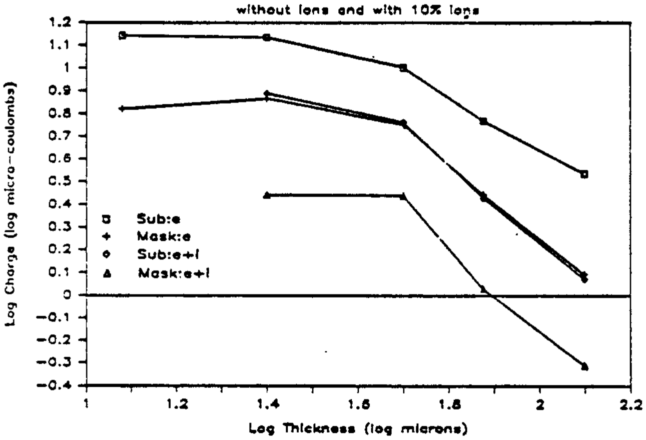

Fig.1(b) *TEFLON MAXIMUM CHARGE*

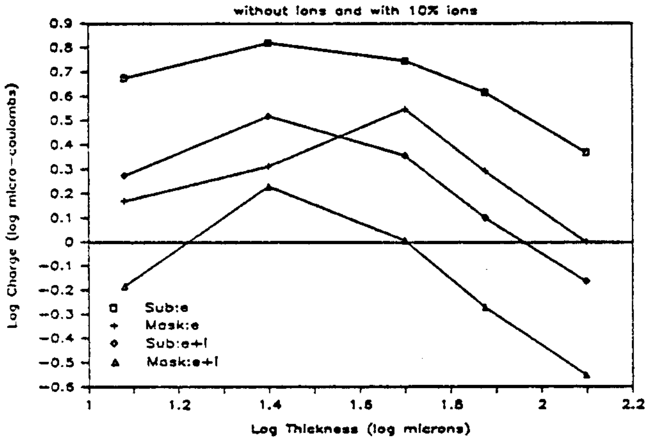

Fig.1(c) *KAPTON MAXIMUM CHARGE*

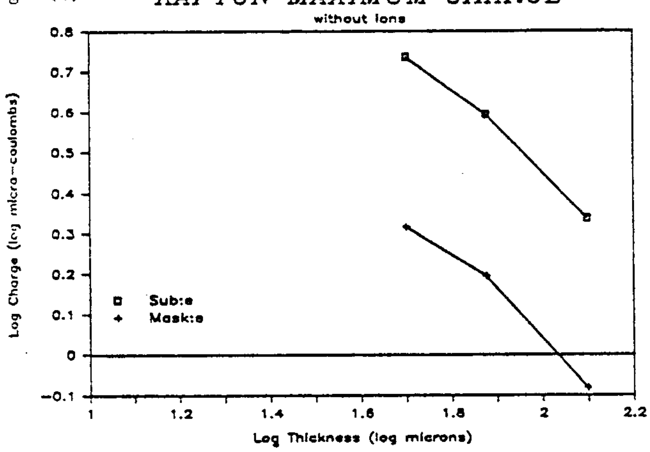

Fig.2(a) *MYLAR MAXIMUM ENERGY*

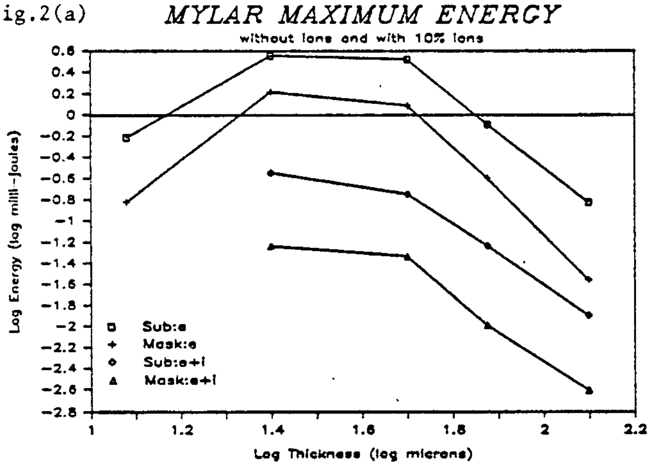

Fig.2(b) *TEFLON MAXIMUM ENERGY*

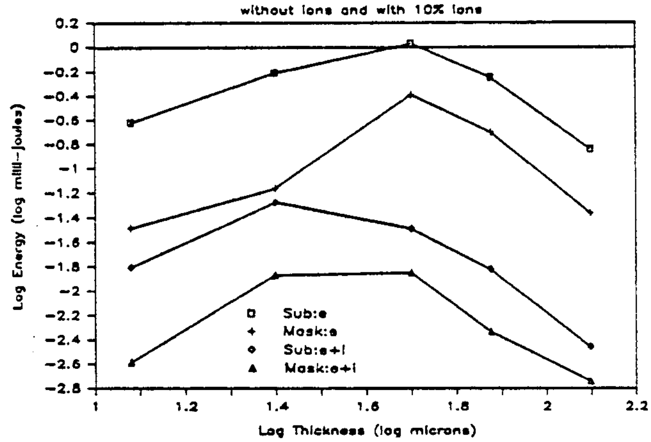

Fig.2(c) *KAPTON MAXIMUM ENERGY*

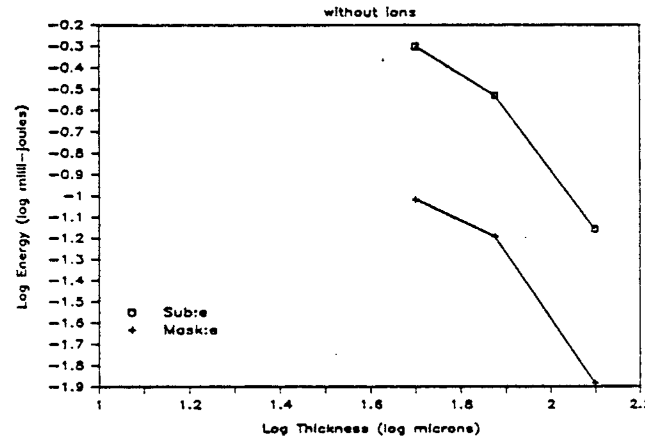

Fig.3(a) *MYLAR MAXIMUM CURRENT PEAKS*

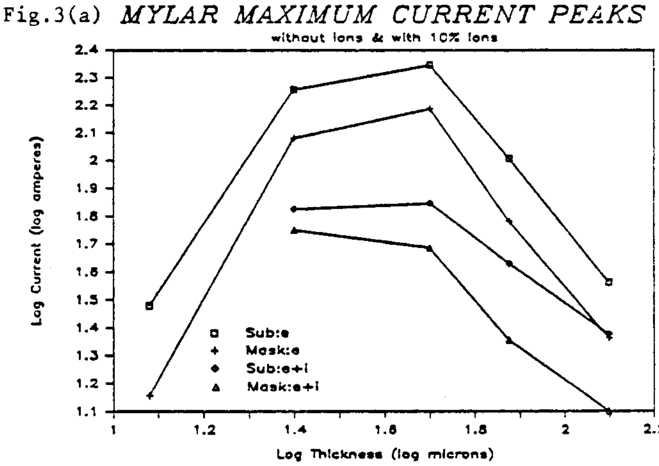

Fig.3(b) *TEFLON MAXIMUM CURRENT PEAKS*

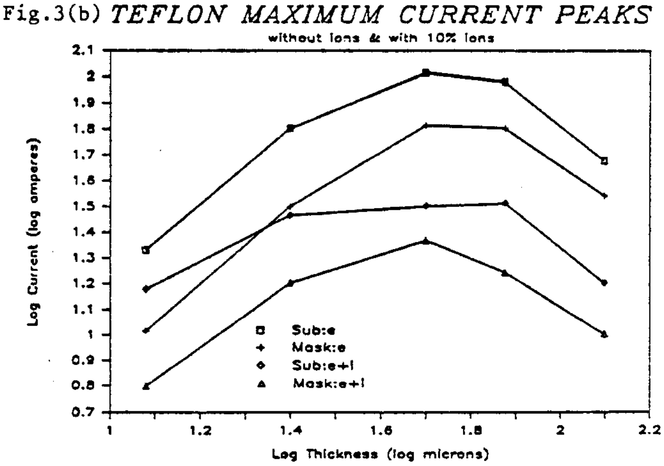

Fig.3(c) *KAPTON MAXIMUM CURRENT PEAKS*

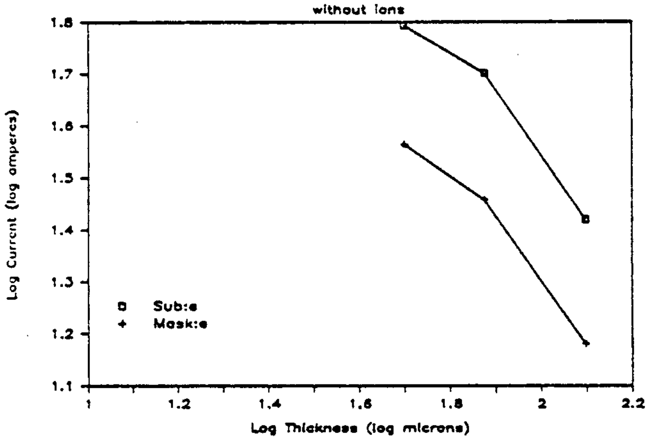

Fig.4(a) *MYLAR PULSE DURATION*

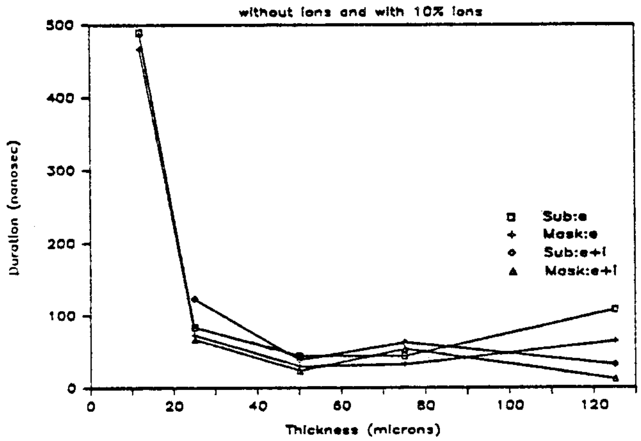

Fig.4(b) *TEFLON PULSE DURATION*

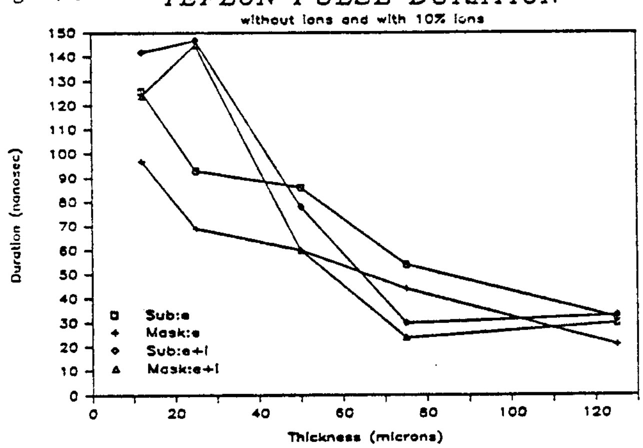

Fig.4(c) *KAPTON PULSE DURATION*

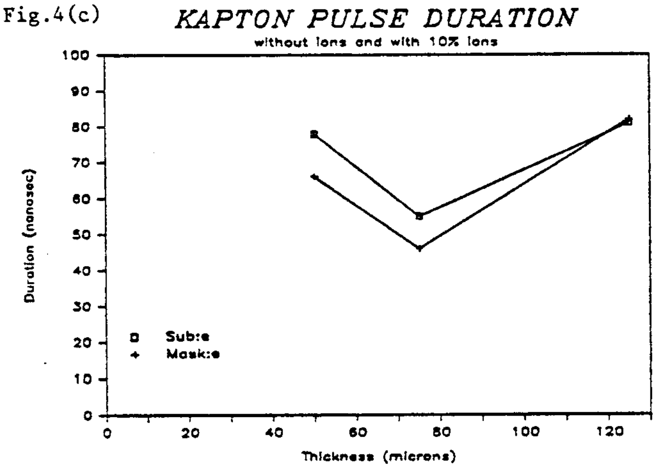

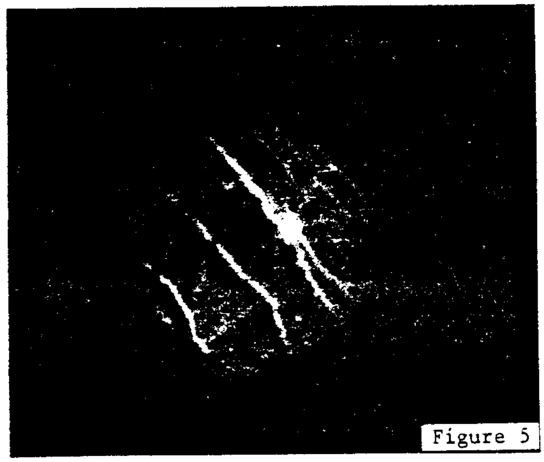

Figure 5

Figure 6

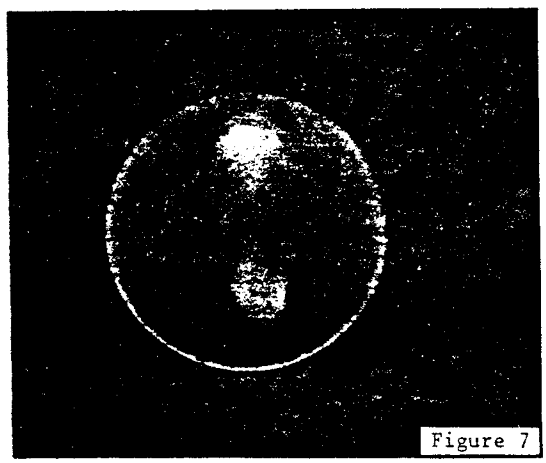

Figure 7

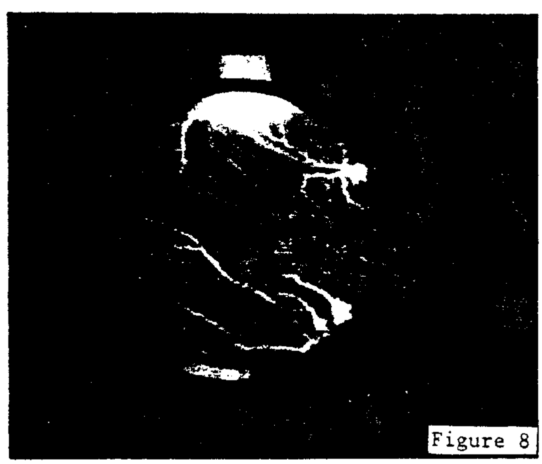

Figure 8